CHAPTER 5

Effects of Tropical Mountain Elevations on the Climate of the Late Carboniferous: Climate Model Simulations

Bette L. Otto-Bliesner

The Westphalian (~305 million years ago [Ma]), during the Late Carboniferous, is interesting from both a geologic and a climatic standpoint. The southern supercontinent of Gondwana and the tropical continent of Laurussia had collided closing the seaway that had separated them during the Devonian and the Earlier Carboniferous (Ziegler et al., 1979; Scotese, 1994). As a result of this collision, the Central Pangean Mountains, consisting of the Appalachian-Mauretanide-Hercynian orogenic belts, formed at tropical latitudes. Based on high-temperature/high-pressure metamorphics found for the late

Paleozoic Appalachian mountains, these mountains probably reached over 3 km in altitude (Ziegler et al., 1985).

The Westphalian was also the time when the extensive coal deposits of eastern North America, western Europe, and the Donetz Basin of the Ukraine formed in the (then) tropical zone between 12°S and 10°N (Fig. 5.1) (Ronov, 1976; Parrish et al., 1986). The presence of these coal deposits has been cited as evidence of a broad latitudinal band of tropical wetness (Raymond et al., 1989). The prerequisite for tropical coal deposits: luxuriant
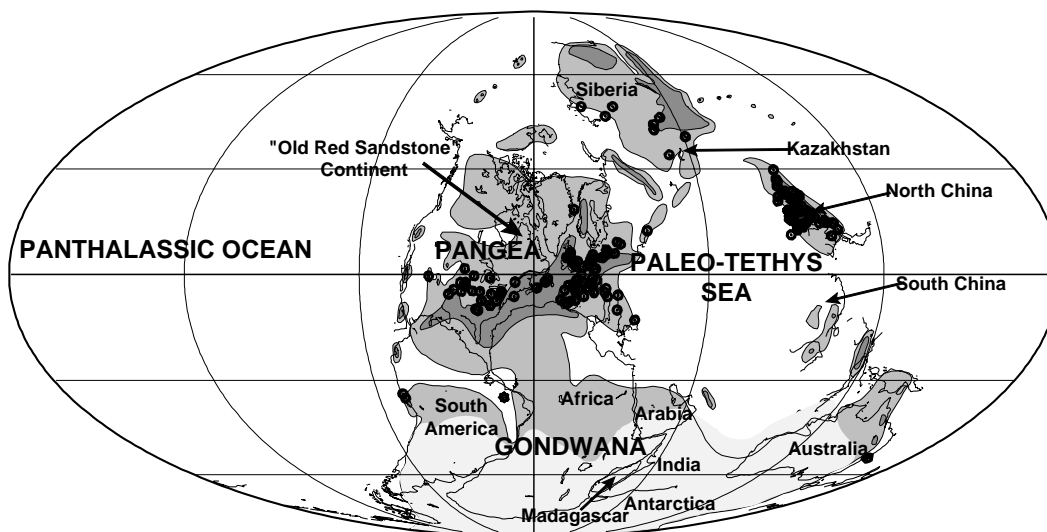

Fig. 5.1. Evidence for extensive Carboniferous coal deposits (Kraus et al., 1993) in the tropical zone between 12°S and 10°N along the northern flank of the Central Pangean Mountains. Figure illustrates Westphalian (Late Carboniferous; ~305 Ma) paleogeography and present-day continental outlines (Scotese, 1994). Shading and symbols: dark gray = mountains, medium gray = lowlands, light gray = land ice, white = oceanic areas, •'s = coals.

plant growth, swamp formation, and peat preservation, are at present generally met in only a narrow latitudinal band about the equator with monthly continuity of rainfall (Ziegler et al., 1987). Studies of well-preserved wood in Westphalian deposits reveal either faint or no growth rings indicating that the growth of the coal floras was not interrupted by seasonal dry spells (Creber and Chaloner, 1984; Chaloner and Creber, 1990).

Topography is known to be an important climatic control (Meehl, 1992). Careful attention needs to be given to prescription of paleotopography in modeling climate on tectonic time scales. Hay et al. (1990), using a pole-to-pole idealized continent with a north-south mountain range as the lower boundary condition in a Global Climate Model, found zonal patterns of continental precipitation and soil moisture and concluded that the present-day nonzonal climatic patterns may be related to large asymmetric topographic features such as the Himalayan-Tibetan Plateau complex. This mountain complex in southern Asia is known to enhance the summer Asian monsoonal circulation and precipitation. With a much lower Tibetan Plateau (Ruddiman and Kutzbach, 1990), a condition which existed before the Neogene, GCM simulations give a much weaker summer monsoon system (e.g., half-mountain (HM) results, Kutzbach et al., 1989; Ruddiman and Kutzbach, 1989) . The uplift history of this plateau remains fragmentary although uncertainties are being reduced through application of a variety of methodologies (Harrison et al., this volume, chapter 3).

The extensive Central Pangean Mountain Belt has been proposed as a possible focus of year-round precipitation over the broad tropical zone of Westphalian coal formation, in particular, on the windward side of the mountain belt (Rowley et al., 1985). No present-day analogs exist for this tropical mountain belt. Present-day mountains at tropical latitudes occupy a much smaller areal extent and are significantly lower. The Himalayan-Tibetan Plateau complex is at subtropical to mid-latitudes. The simulations in this study are undertaken to provide an assessment of the thermodynamic and dynamic response of the atmosphere to an extensive tropical mountain belt. In particular, the sensitivity of the response to the elevation of the mountain belt is investigated. These simulations illustrate the importance of accurate reconstructions of paleotopography in applying global climate models to paleoclimate problems.

Details of Numerical Model

A set of sensitivity simulations for the Late Carboniferous was conducted using the National Center for Atmospheric Research (NCAR) GENESIS Global Climate Model, version 1.02 (Thompson and Pollard, 1995). The model consists of components for the atmosphere, ocean, and land-surface. The atmospheric component is based on the NCAR Community Climate Model version 1 (CCM1). The atmosphere is described by the equations of fluid motion, thermodynamics, and mass continuity along with representations of radiative and convective processes, cloudiness, precipitation, and the influence of mountain belts. The CCM1 code has been modified to incorporate new model physics for solar radiation, water vapor transport, convection, boundary layer mixing, and clouds. The horizontal resolution is R15 which corresponds to a 4.5° latitude by 7.5° longitude spectral transform grid, on average. A sigma-coordinate system is used in the vertical with 12 levels.

The ocean component of GENESIS contains a 50-meter deep mixed-layer ocean coupled to a thermodynamic sea-ice model. The ocean representation crudely captures the seasonal heat capacity of the ocean mixed layer but ignores salinity, upwelling, and energy exchange with deeper layers. Poleward oceanic heat transport is included in present-day simulations using the prescribed latitudinal variation from the "0.5 x OCNFLX" case of Covey and Thompson (1989). A six-layer sea-ice model, patterned after Semtner (1976), predicts local changes in sea ice thickness through melting of the upper layer and freezing or melting on the bottom surface. Fractional sea ice coverage is included, as is a reduction in the albedo as the surface temperature of the sea ice approaches 0°C.

The land-surface component (Pollard and Thompson, 1995) incorporates a land-surface transfer model (LSX) which accounts for the physical effects of vegetation, a three-layer thermodynamic snow model, and a six-layer soil model. The soil model layers are chosen so that the top layer is thin enough (5 cm) to capture diurnal temperature variations, while the total thickness (4.25 m) is capable

of resolving seasonal variations. Heat is diffused linearly and moisture nonlinearly, with a provision for soil ice. Water can infiltrate into the soil at a rate capped by the rate of downward soil drainage and diffusion in the upper layer. Any excess rainfall minus evaporation and any excess snowmelt become surface runoff.

The GENESIS model adequately reproduces observed present-day patterns of precipitation over tropical land with the Intertropical Convergence Zone (ITCZ) precipitation maximum centered at 10°S latitude in January shifting northward to 8°N in July (Thompson and Pollard, 1995). Soil moisture patterns and their seasonal variations are strongly controlled by the model precipitation. The model's global and annual mean precipitation (4.5 mm day^{-1}) is considerably greater than observed (3.1 mm day^{-1}). The zonal mean values are approximately 60% greater than observed because of high precipitation associated with ITCZ convection. This overestimate occurs over both land and ocean but is a bias in only the magnitude not the location of the precipitation maxima. It has been corrected in a newer version of GENESIS with decreased surface drag over oceans.

Climate Sensitivity Simulations and Boundary Conditions

The sensitivity of the Late Carboniferous tropical climate was examined in a series of sensitivity simulations exploring the effects of four different tropical mountain elevations (Table 5.1). The baseline Carboniferous simulation (hereinafter referred to as TMNONE) was performed with tropical land elevations uniform at 0.5 km. The sensitivity simulations involved progressively elevating the Central Pangean Mountains to test the sensitivity of the tropical climate to uncertainties in the reconstructed height of these mountains. All other boundary conditions are kept the same in the simulations (Table 5.2).

Paleogeography and Topography

Paleogeography for the model simulations adopted the ~305 Ma reconstruction (Fig. 5.1) of C.R. Scotese and J. Golonka (Scotese, 1994). The plate tectonic reconstruction is based primarily on the paleomagnetic data compiled by Van der Voo

Table 5.1. Topography Specification

Experiment	Prescribed Values
Tropical No Mountain TMNONE	500 m lowlands 500 m tropical mountains
Tropical Low Mountain TMLOW	500 m lowlands 1000 m tropical mountains
Tropical Mountain TMREAL	500 m lowlands 1000–3000 m tropical mountains
Tropical High Mountain TMHIGH	500 m lowlands 5000 m tropical mountains

(1993) with modifications over Siberia (Khramov and Rodionov, 1980). The Late Carboniferous marks the beginning of the formation of Pangea. The southern supercontinent of Gondwana, consisting of South America, Africa, Australia, Antarctica, and parts of Asia, and the tropical continent of Laurussia, made up of North America and parts of Eu-

Table 5.2. Boundary Conditions for GENESIS Model Simulations (see text and figures for details)

Boundary Conditions	Prescribed Values
Solar luminosity	1328.9 W m^{-2} (3% less than present)
Orbital parameters eccentricity/obliquity/ precession	0 / 23.4° / 0
Atmospheric CO_2	Present-day
Ozone mixing ratio	Present-day
Land-sea distribution	Scotese (1994) (Fig. 5.1)
Topography	Table 5.1, Fig. 5.2
Land ice	South Pole to ~45°S 500–3000 m elevation (Figs. 5.1 and 5.2)
Soil characteristics texture/color	Intermediate between sand and clay / Intermediate
Vegetation type	No vegetation—bare soil
Oceanic poleward heat flux	Present-day averaged to be symmetric about equator

rope, had collided closing the seaway that had separated them earlier. As a result of this Himalayan-type collision, a large tropical mountain range was formed. Data also indicate mountainous belts over the Northern Hemisphere land masses and at high southern latitudes. In these simulations, nonmountainous land is set to an elevation of 0.5 km, while mountain ranges outside the tropics are assigned elevations ranging up to 3 km using topographic and plate tectonic analogs (Ziegler et al., 1985).

With a Himalayan-type collision between Gondwana and Laurussia, considerable uplift is conceivable but large uncertainties exist. Tropical mountain heights were thus varied among the simulations. In the TMNONE simulation, tropical mountain heights were set to 0.5 km, the same as the surrounding lowlands. The TMLOW, TMREAL, and TMHIGH simulations prescribe successively higher elevations to the tropical mountain range (Table 5.1). The TMREAL simulation allows variation in the height of these mountains and is considered the most "realistic." The TMHIGH simulation is an extreme orography run. The model representation (spectrally smoothed to R15 resolution) of the land elevations is given in Figure 5.2.

These initial sensitivity simulations all assume no vegetation and soil with texture intermediate between sand and clay and with intermediate color. At ocean points, poleward oceanic heat transport was modified for the Late Carboniferous simulations by
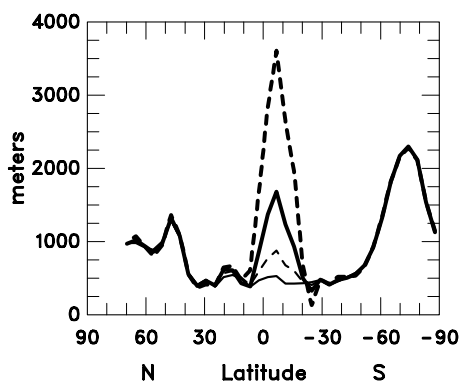

Fig. 5.2. Comparison of model representation of land elevations (in meters). Figure illustrates latitudinal distribution, averaged for continental areas only, for TMNONE (thin solid), TMLOW (thin dashed), TMREAL (heavy solid), and TMHIGH (heavy dashed) simulations. The TMREAL simulation is considered the most realistic based on topographic and plate tectonic analogs.

averaging Covey and Thompson's (1989) data to make it symmetric about the equator.

Ice Sheet and Snowcover

Glacial deposits (tillites) dated to the Late Carboniferous have been found on the continents of Australia, Africa, South America, and Antarctica as well as India (Crowell, 1983; Caputo and Crowell, 1985; Veevers and Powell, 1987) and suggest the possibility of four ice sheets with total areal extent of 18 $\times$ 10^6 km^2 (Parrish et al., 1986; Veevers and Powell, 1987; Crowley and Baum, 1991). A more extensive single ice sheet covering nearly 70% of the continent of Gondwana from the South Pole to roughly 45°S latitude and with areal extent of 42 $\times$ 10^6 km^2 has been proposed by Scotese and Golonka (personal communication, 1993). The rationale for a single massive ice sheet assumes extensive destruction of glacial evidence, especially during highly erosional post-glacial environments. This proposed glacial ice reconstruction gives an estimated glacio-eustatic sea level fluctuation of 190 m which is on the high end of the range of sea level estimates (70–200 m) from cyclothem fluctuations (Crowley and Baum, 1991). For comparison, the area of the Laurentide ice sheet at 21,000 BP is estimated to be about 12 $\times$ 10^6 km^2 (Crowley and Baum, 1991). This extensive ice sheet was prescribed in all simulations (Fig. 5.1) and ice-sheet heights ranging up to 3 km were assigned using the area-volume relationship employed in the CLIMAP studies (Paterson, 1972) (Fig. 5.2).

Atmospheric Carbon Dioxide

Models of the geochemical cycle (Walker et al., 1981; Garrels and Lerman, 1984; Budyko et al., 1987; Berner, 1994) and independent isotopic measurements of paleosols (ancient soils) (Mora et al., 1996) and marine sediments (Freeman and Hayes, 1992; Yapp and Poths, 1992) suggest that atmospheric CO_2 has varied considerably over the last 600 m.y. because of imbalances in the effects of weathering, organic burial, and metamorphism. A geochemical model of Berner estimated atmospheric CO_2 levels as high as 17 times present concentrations for the Phanerozoic (Berner, 1994). For 305 Ma atmospheric CO_2 concentrations are predicted to be similar to the present (Berner, this volume,

chapter 12). Input of CO_2 into the atmosphere by global degassing might have been low if seafloor spreading rates diminished with the formation of Pangea, while a significant draw down of atmospheric CO_2 is expected to have occurred between 380 and 350 Ma in response to enhanced burial of organic carbon as a consequence of the rise and spread of vascular land plants (Berner, this volume, chapter 12). Atmospheric CO_2 concentrations equal to those in the present-day control run of GENESIS (340 ppm) were adopted for these simulations.

Solar Luminosity

The solar constant can vary because of changes in the sun's output and the Earth's orbital dynamics. Astrophysicists calculate that the sun has brightened over the age of the Earth (~ 4.6 billion years), as hydrogen has been converted to helium in the sun's core (Endal and Sofia, 1981), having been 30–40% dimmer when the Earth formed. Over the Phanerozoic, this translates to an approximate 6% increase in solar luminosity (Crowley et al., 1991). The solar luminosity at 305 Ma has been set to 3% less than present (present-day value: 1370 W m^{-2}) in all simulations. Milankovitch cycles of the Earth's orbital dynamics have been documented in records for the Pleistocene, but the periods and magnitude of this forcing before the Pleistocene are uncertain (Berger, 1978; Berger et al., 1989). A circular solar orbit (eccentricity = 0) with present-day obliquity (23.4°) is therefore assumed. This orbital configuration omits any differences in solar forcing between the Northern and Southern Hemispheres in their respective seasons.

Climatology of the Tropics at Present

The present-day tropical climate between 30°S and 30°N is influenced by the equatorial low pressure belt, the subtropical highs, and the trade winds. Near the equator, the climate is characterized by high humidity and cloud cover and daily showers of heavy, localized rainfall. Warm temperatures and abundant rainfall year-round combine to favor dense, broadleaf, evergreen forest vegetation. Rainfall in these regions is the result of the converging air flow of the trade winds from the North- and Southern Hemispheres into the equatorial low pressure belt. This convergence forces warm, moist,

unstable air upward forming clouds and generating showers. This narrow zone of converging air is termed the ITCZ. Subtropical high pressure belts of subsiding air, clear skies, and sparse precipitation dominate at 25–30° latitude.

Because of the tilt of the Earth's axis with respect to the Earth's orbital plane, the sun is more directly overhead in the Northern Hemisphere in July and in the Southern Hemisphere in January. The zone of maximum surface heating in the tropics shifts seasonally with it. In response, the major pressure systems and wind regimes affecting tropical climate shift north in July and south in January. Thus, the ITCZ and associated abundant rainfall is concentrated north of the equator at ~5–10°N in July and south of the equator at ~5–10°S in January (Fig. 5.3). The region that receives abundant rainfall year-round is thus confined to a band 8–10° wide near the equator (Fig. 5.4). On either side of this rainforest zone, a wet summer–dry winter climate prevails because of the seasonal shifts of the ITCZ and subtropical highs which alternate in controlling the precipitation regime (Fig. 5.3).

Results of Sensitivity Experiments

The TMREAL simulation was started from a zonally-symmetric wind and temperature initial state and integrated through 18 seasonal cycles. Approach to equilibrium is discussed in Otto-Bliesner (1996). All other simulations were started from year 12 of the TMREAL simulation and integrated for 6 years. Mean climate statistics represent 5-year averages calculated from years 14–18 of the simulations. The standard deviation of the monthly average statistics for the individual years from the 5-year average is also computed. This is a measure of the interannual variability inherent in the model statistics. The standard deviations can be used in conjunction with the Student *t*-test (Panofsky and Brier, 1965) to separate signal from noise (Chervin and Schneider, 1976) when comparing simulations. For this set of simulations, the difference between two simulations is statistically significant at the 95% level if the change is greater than 1.75 times the standard deviation. That is, there is 5% chance that this difference could occur by chance. Those differences less than this limiting value are not considered statistically different and fall within the year-to-year variability of the model results.
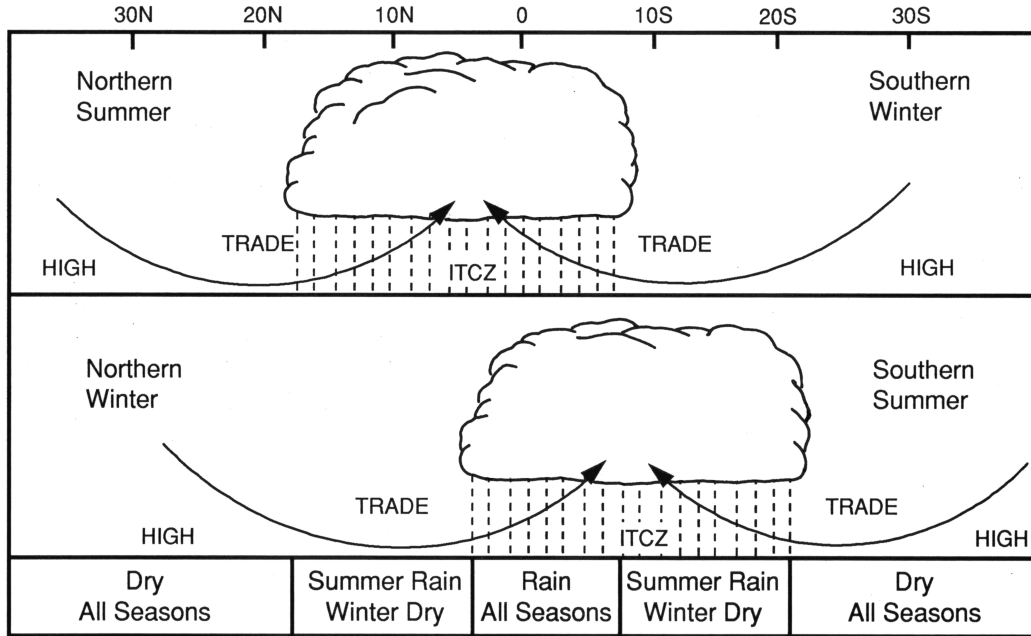
Fig. 5.3. Schematic of pressure and air flow and resultant precipitation during the course of the year. Migration of zone of tropical convergence and rising air into summer hemisphere results in zones of winter dryness banding the tropical everwet zone (Adapted from Trewartha and Horn, 1980).
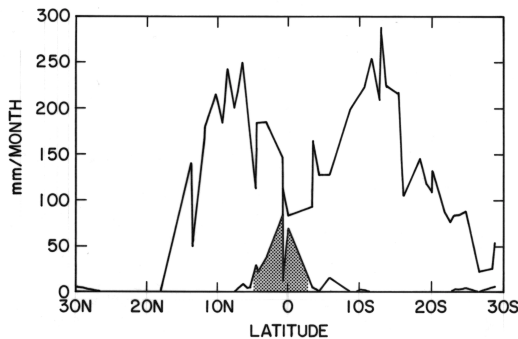

Fig. 5.4. Present-day observed January and July rainfall versus latitude for Africa. Note that the position of the ITCZ and thus maximum rainfall is located at 13°S in January and 6°N in July resulting in only a narrow band at the equator (3°S–5°N) where precipitation is greater than 20 mm in both months. (After Ziegler et al., 1987)

The tropical surface patterns and hydrologic response are strongly influenced by the latitudinal migration of the sun with seasons. Small changes in surface heating lead to substantial excursions of surface convergence and precipitation. The location of the Central Pangean Mountains just south of the equator result in these mountains having their largest effect during the boreal summer (June–July–August) when maximum solar heating occurs north of the equator. Model comparisons for July will thus be emphasized.

Temperature

Increasing the elevation of the Central Pangean Mountains significantly cools July surface temperatures over the mountainous areas (Fig. 5.5). In the TMNONE simulation (Fig. 5.5a), July surface temperatures at 7°S over land average 18°C, a cooling of 5°C compared to the present because of the low-

ered solar luminosity at 305 Ma. Raising the mountain heights from 0.5 to 1 km further lowers July temperatures over elevated tropical land by ~2°C in the TMLOW simulation, a statistically significant cooling compared to the small interannual temperature variability at these latitudes (Figs. 5.5b). The "realistic" mountain heights in the TMREAL simulation lead to a pronounced cooling of up to 14°C (Fig. 5.5f), although July temperatures remain above freezing even over the highest elevations (Fig. 5.5c). Temperature gradients on the northern side of the mountains are greatly enhanced. July temperatures are below freezing over the higher elevations in the TMHIGH simulation with surface temperatures as low as -20°C and average land temperatures at 7°S of -4°C (Figs. 5.5d, 5.5g). Cooling over the higher elevations is significant in all simulations, but these changes are local. Significant remote changes in temperature do not develop. These results are in accord with an effective length scale of temperature perturbations of ~1500 km found in previous modeling studies (North et al., 1992; Crowley et al., 1994) .

Sea Level Pressure and Surface Winds

Temperature changes induced by the Central Pangean Mountains induce changes in the July sea level pressure patterns over the tropical land areas and force changes in the surface wind patterns (Fig. 5.6). In the TMNONE simulation, the equatorial low pressure belt follows the sun shifting north of the equator in July (Fig. 5.6a). Surface flow is predominantly from the east with appreciable cross-equatorial surface flow from the Southern to the Northern Hemisphere (Fig. 5.6e). Convergence of the surface winds place the ITCZ at approximately 20°N latitude. Onshore flow from the eastern Panthalassa Ocean at 5°N leads to weak surface convergence into the east-west oriented trough of low pressure.

The addition of mountains over the tropical land areas affects the seasonal excursion of the equatorial low pressure belt and thus the regions of surface convergence. In the TMLOW simulation the effect is small (Figs. 5.6b, 5.6f). Much larger changes occur in the TMREAL simulation (Figs. 5.6c, 5.6g). A band of low pressure and resulting surface convergence over the tropical continental area is still located north of the equator, but a pronounced trough

of low pressure also extends southwestward along the northern edge of the Central Pangean Mountain Range, which serves as an elevated heat source in July. As a result, strong low-level convergence into this low pressure system from both the eastern and western Panthalassa Ocean occurs in the vicinity of the mountains. Large gradients in the prescribed topography in the TMHIGH simulation result in less organized (and noisier) patterns in sea level pressure in their vicinity (Fig. 5.6d), although the general pattern is similar to the TMREAL simulation. In addition, surface flow is disrupted with cold, downslope flow along the southern edge of these high mountains (Fig. 5.6h).

Vertical Motion

Surface convergence patterns can be better delineated by examining vertical motion fields. In Figure 5.7, latitudinal cross sections of vertical motion along 0° longitude give the predicted vertical motion from the surface to the top of the atmosphere. This longitude transects the Central Pangean Mountains and the region of tropical coal deposits. The shift of the ITCZ north of the equator in July in the TMNONE and TMLOW simulations leads to maximum upward motion at 12°N (Figs. 5.7a, 5.7b). Sinking motion occurs south of the equator. Upward vertical motion covers a much broader latitudinal band in the TMREAL and TMHIGH simulations extending from 20°N to 10°S as the mountains force converging surface flow upward (Figs. 5.7c, 5.7d).

Precipitation

Maximum precipitation (Fig. 5.8) over the tropical land areas coincides with regions of maximum surface convergence and upward vertical motion. In the TMNONE simulation, a band of precipitation extends from 5°N over western Laurussia to 15°N over eastern Laurussia (Fig. 5.8a). Little precipitation falls from 5–25°S. Although precipitation increases over tropical land areas in July in the TMLOW simulation, the changes are not significant (Figs. 5.8b, 5.8f). Raising the mountain peaks to 2–3 km elevation significantly enhances upslope precipitation on the northern flanks of the Central Pangean Mountains (Figs. 5.8c, 5.8e, 5.8g). The precipitation pattern has a bimodal distribution with a band of precipitation (continental average of
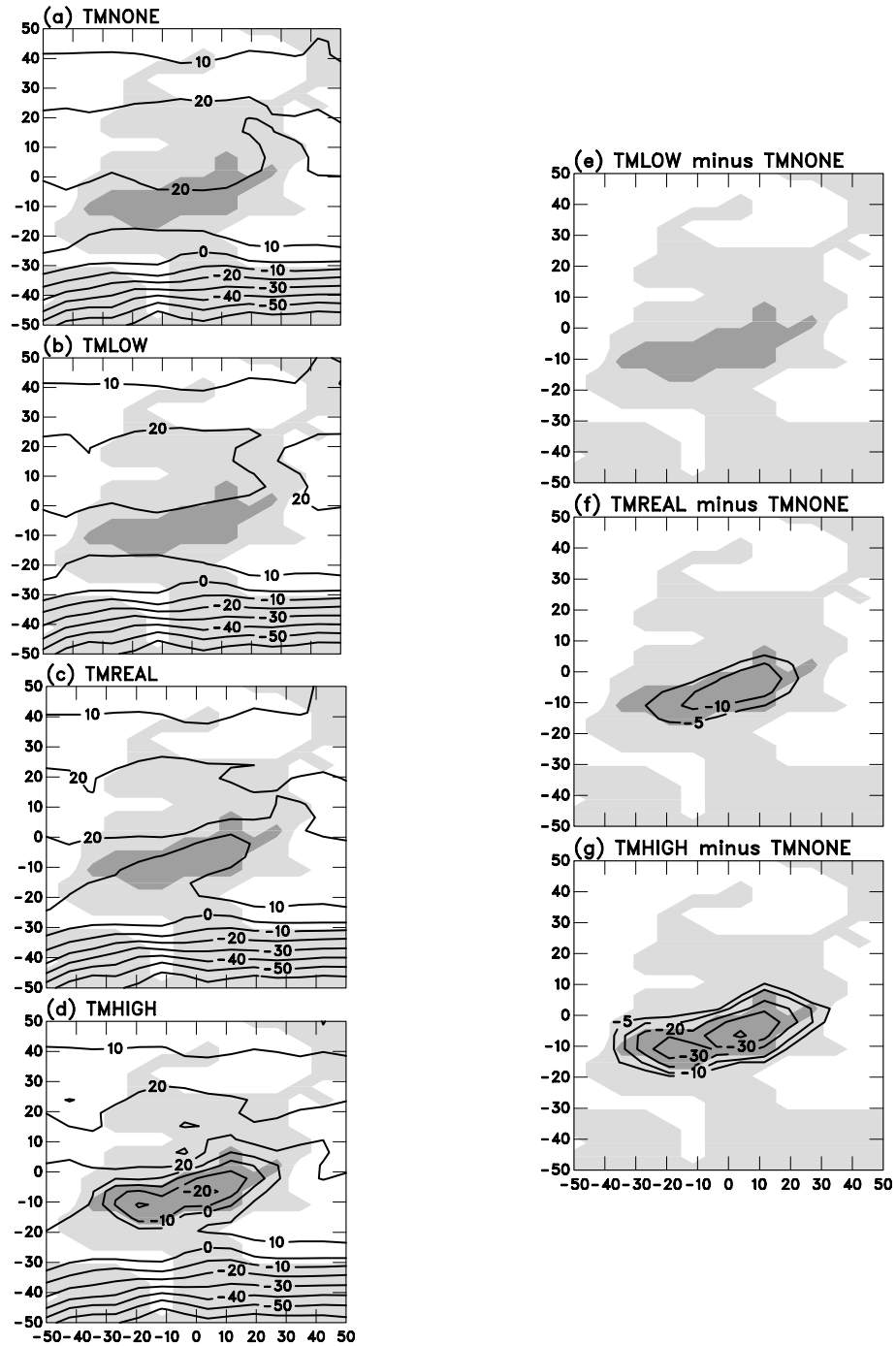
EFFECTS OF TROPICAL MOUNTAIN ELEVATIONS ON CLIMATE

Fig. 5.5. Comparison of July surface air temperatures (°C) (temperature at 2 m above the surface in the model simulations). The elevations of the tropical mountains in the TMREAL and TMHIGH simulations result in substantial cooling in their vicinity. Surface temperatures remain below freezing year-round over the higher elevations in the TMHIGH simulations. The location of the Central Pangean Mountains is shaded.

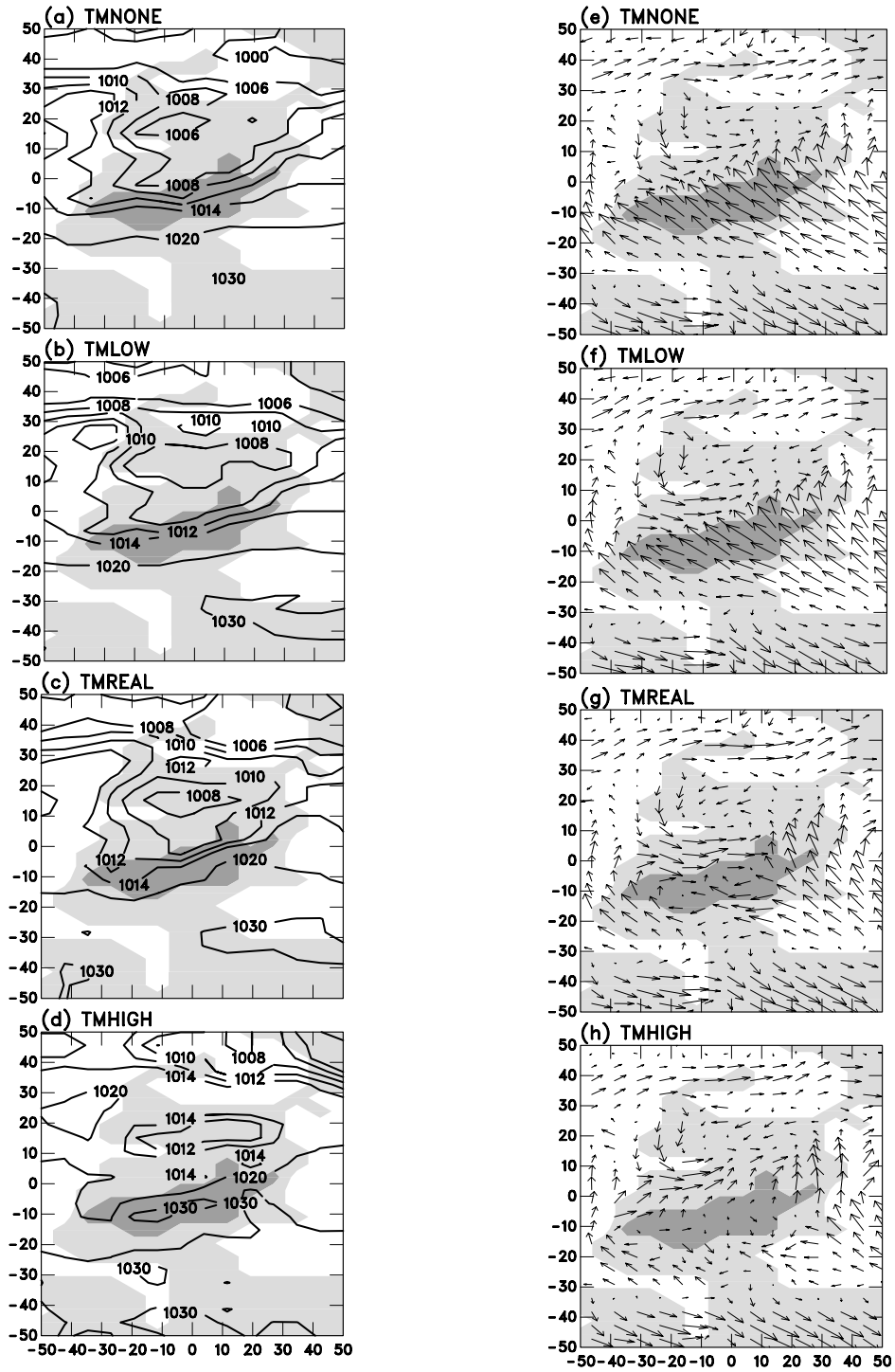**Fig. 5.6.** Changes in the July sea level pressure (mb) patterns force changes in the surface wind patterns (vector length: 1°/1 m s⁻¹). Strong cross-equatorial flow from the Southern to Northern Hemisphere dominates in the TMNONE and TMLOW simulations. Greater mountain heights in the TMREAL simulation induce converging surface winds on the northern edge of the Central Pangean Mountains but leads to unrealistic downslope winds in the TMHIGH simulation.
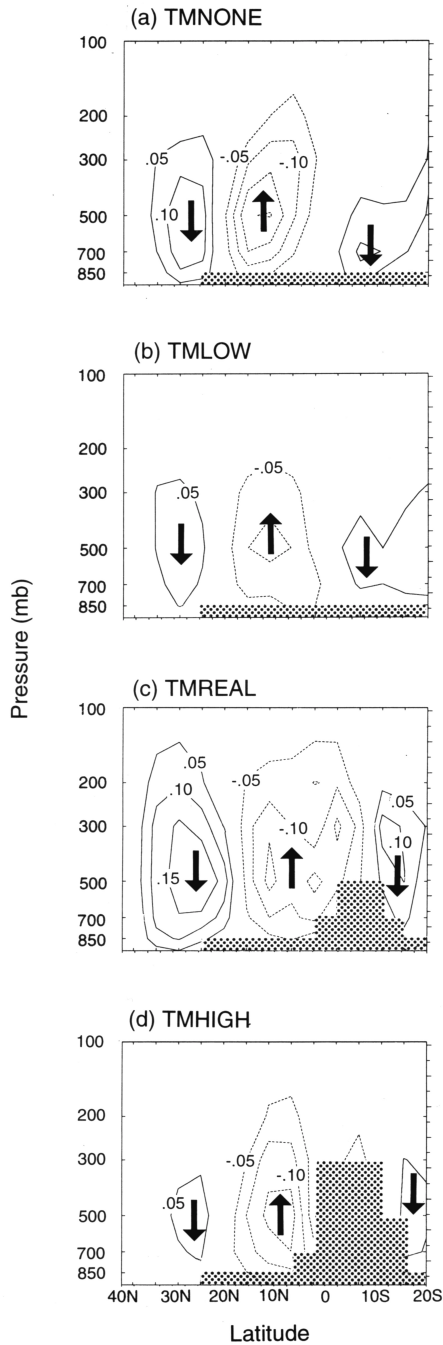
Fig. 5.7. Converging surface winds in the tropics result in rising vertical motions. Figure shows latitudinal cross-sections of vertical motion (Pa s^{-1}, negative indicates upward motion) in July at 0° longitude. Rising air occurs at 10–15°N in July in all the simulations. The higher mountains in TMREAL and TMHIGH induce rising motion at 0–5°S (the northern flank of the Central Pangean Mountains), a region of sinking air in July in the TMNONE and TMLOW simulations.

9 mm/day at 10°N) associated with the main portion of the ITCZ north of the equator and a localized maximum of precipitation (continental average of 6 mm/day) over the northeastern flanks of the mountains. Precipitation decreases north of the latter maximum although not significantly. These precipitation decreases are more pronounced in the TMHIGH simulation and significant along the coastal regions at 10°N (Figs. 5.8d, 5.8h). Because of the disruption of low-level flow patterns by the unrealistically steep mountains prescribed in the TMHIGH simulation, the precipitation increases along the northern edge of the mountains in a less well-organized but still significant way.

Soil Moisture

Soil moisture predictions by the model give the time-integrated effects of precipitation and evaporation on the surface moisture (Fig. 5.9). July soil moisture is moderate to high along the eastern tropical coastlines of the Westphalian continent in the TMNONE simulation but is very low in the interior regions south of the equator (Fig. 5.9a). Soil moisture increases in the western regions, in the TMLOW simulation, but is still low (Fig. 5.9b). Increased precipitation along the northern flanks of the mountains in the TMREAL simulation results in significantly increased soil moisture in those regions (Fig. 5.9c). The soils in western Laurussia are still quite dry south of the equator. Although precipitation does not increase as greatly in the TMHIGH simulation as in the TMREAL simulation, soil moisture is significantly enhanced with a broad region > 80% as a result of significantly decreased evaporation over these mountainous regions with their cold surface temperatures (Fig. 5.9d). Soil moisture in these regions consists of ice crystals in the soil pores. The TMHIGH simulation gives unrealistically low soil moisture over eastern Laurussia north of the equator.

Seasonal Variation

The coals of the Westphalian are thought to have been formed under conditions of year-round wetness (Ziegler et al., 1987; Chaloner and Creber, 1990). In figure 5.10, the seasonal variation of precipitation, evaporation, and soil moisture on the north-
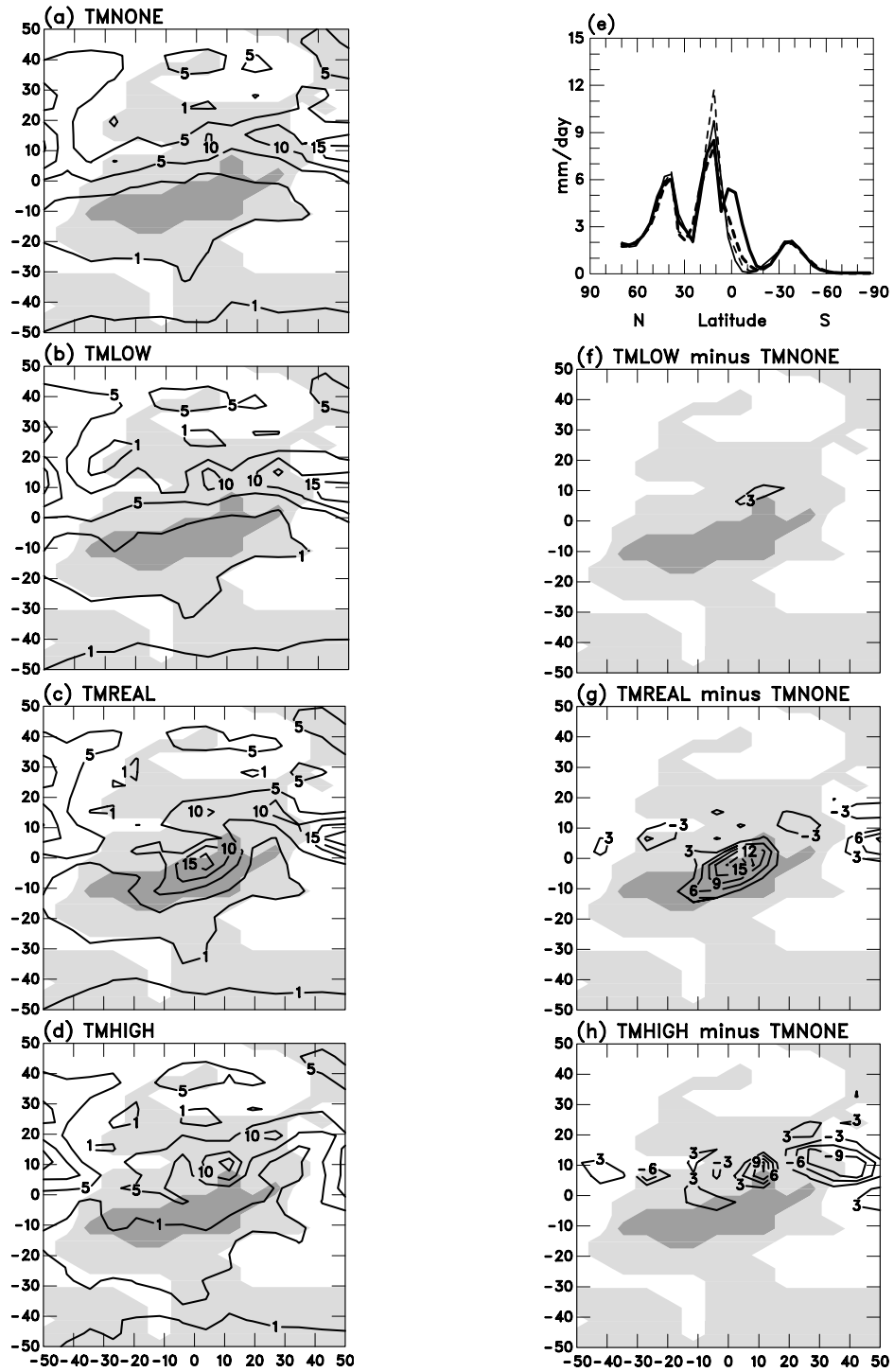
Fig. 5.8. Changes in July precipitation (mm/day) in the model simulations. Converging surface flow and rising motion at 0–5°S in the TMREAL simulation significantly enhances precipitation. The actual precipitation amounts are given in (a) – (d) with precipitation differences from the TMNONE simulation given in (f) – (h). The average continental precipitation as a function of latitude is given in (e). See Fig. 5.2 for legend.
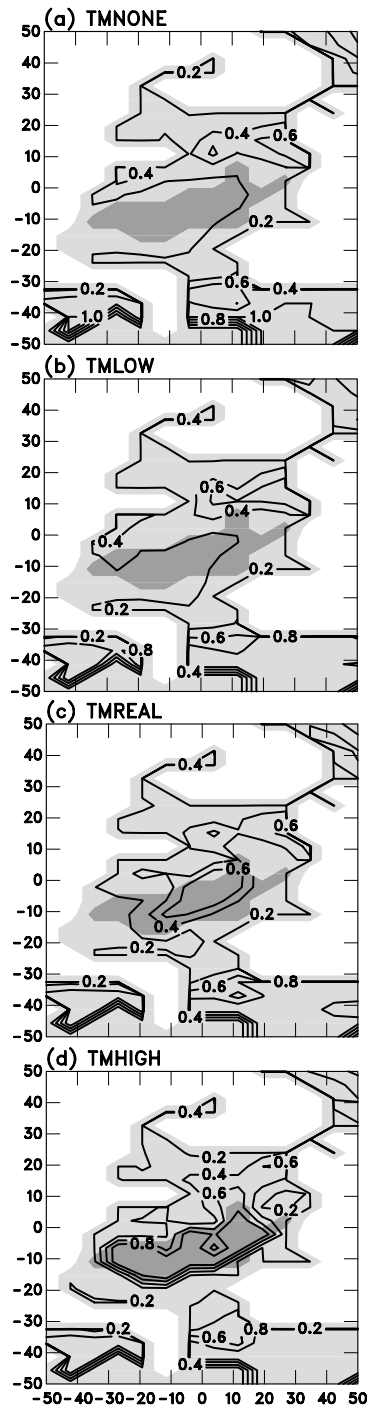
Fig. 5.9. July soil moisture (fractional amount) indicates dry conditions in the tropical band just south of the equator in the TMNONE and TMLOW simulations. Enhanced precipitation in the TMREAL simulation and much cooler temperatures in the TMHIGH simulation result in wetter soil conditions over the Central Pangean Mountains.

ern edge of the mountains (latitude 2.3°S, longitude 0°) delineates how well each simulation meets this requirement. In the TMNONE simulation, precipitation, evaporation, and soil moisture all exhibit large seasonal cycles with maximum amounts from November–March and minimum amounts from June–September. Soil moisture varies considerably from a high of 0.5–0.6 in February–March to a low of 0.1–0.2 from June–September. Precipitation is negligible from June–September. The TMLOW simulation also exhibits large seasonal variations. Precipitation increases in this area in September in the TMLOW simulation, but much of this increase is removed from the soils by increased evaporation. Soil moisture exhibits very little seasonal variation
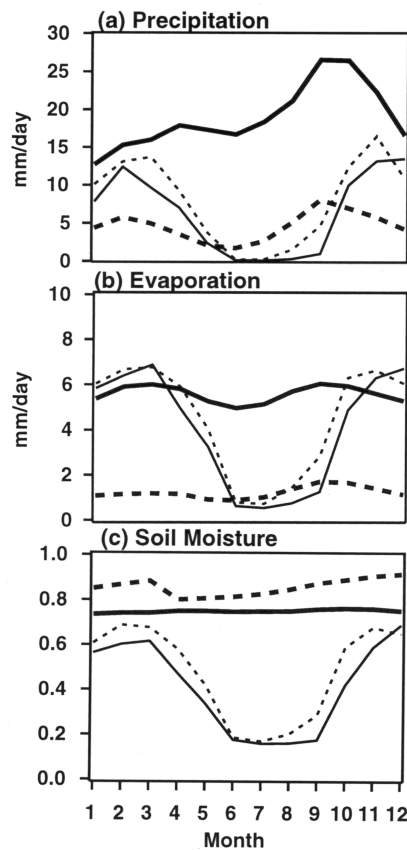

Fig. 5.10. The prescription of mountain heights at 1–3 km in the TMREAL simulations results in flow patterns such that the minima in precipitation, evaporation, and soil moisture in June–July–August in the TMNONE and TMLOW simulations are eliminated. This is consistent with interpretations of year-round wetness in coal-forming regions. This figure shows monthly averages for a locale on the northern edge of the Central Pangean Mountains (2.3°S latitude, 0° longitude). See Fig. 5.2 for legend.

at this location in the TMREAL and TMHIGH simulations averaging 0.75 in the TMREAL simulation and 0.85 in the TMHIGH simulation. Precipitation is greatest in the TMREAL simulation with amounts in excess of 12 mm/day in all months and maximum values during the boreal fall. Precipitation is significantly less in the TMHIGH simulation, but due to greatly reduced evaporation, it is adequate to maintain moist soils.

Discussion and Conclusions

Although accurate determination of land-sea distribution is important for estimating past climates (Fawcett and Barron, this volume, chapter 2), the role of topography also needs to be considered. Because of uncertainties in finding adequate tectonic analogs, precisely determining the height of mountain ranges million of years ago is difficult. These simulations suggest that not only the presence of mountains but the height of the mountains can have a significant effect on the surface flow patterns and hydrologic cycle.

The TMREAL simulation with tropical mountain heights ranging from 1–3 km gives the best fit to the tropical coal data. The Central Pangean Mountains act to impede the seasonal excursions of the Intertropical Convergence Zone. In July, a trough of low pressure remains anchored along the northern edge of the mountains and draws in moisture-laden air from both the western and eastern Panthalassa oceans. This air converges and is forced upward with the uplift enhanced by the mountains. The local increase in July precipitation compared to that predicted in the TMNONE simulation is 680%. Soil moisture remains high year-round in all regions of coal deposits except far western Laurussia. Discrepancies in this region may be due to an underestimation of the mountain peaks in the region. (The TMHIGH simulation with its higher peaks in western Laurussia gives much moister soils in this region.)

Raising the tropical mountain heights to only 1 km in the TMLOW simulation is not adequate to significantly alter the July flow patterns from the TMNONE simulation. The ITCZ shifts north of the equator. Tropical land areas south of the equator are dominated by sinking air and negligible precipitation. Prescribing mountains at too great an elevation and steepness can mask the climatic significance of the mountains. In addition, numeric problems with handling a very steep feature may come into play (Crowley et al., 1994). Sea level pressure patterns become less organized in the TMHIGH simulation disrupting low-level convergence. Precipitation, although enhanced, is less well organized. In addition, downstream effects are more pronounced. Eastern Laurussia at 10°N, a region of considerable coal deposits, receives significantly less precipitation in July and has lower soil moisture in the TMHIGH simulations than in any of the other three simulations.

Similar results are evident for climate model simulations for other time periods during the evolution of the supercontinent of Pangea. By the Permian, the Central Pangean Mountains had shifted to ~10°N with a predominantly east-west orientation (Ziegler, 1990). In climate model simulations, these mountains anchor a lobe of high precipitation year-round increasing precipitation by 25% compared to an idealized Pangea with no topography (Kutzbach and Ziegler, 1993; Kutzbach, 1994). Similarly for the Triassic, Wilson et al. (1994) found that most of the seasonal precipitation in the model falls on the major tropical highlands of Pangea.

The amplification effect of topography on precipitation is dependent on season and the latitudinal location of the mountain range. The Central Pangean Mountains located at tropical latitudes in the Late Carboniferous act to increase local precipitation by 20% in January and 680% in July. The amplification factor in July is tied to the influence of these tropical mountains on the seasonal excursions of the ITCZ. In contrast, climate model simulations with present-day geography suggest that the Tibetan Plateau, located at subtropical to mid-latitudes, enhances summer precipitation in its vicinity by only a factor of 3–4 (Kutzbach et al., 1993). In this case, the subtropical mountains act to enhance the monsoonal circulation associated with the ITCZ rather than its latitudinal excursion. The simulated present-day summer Indian monsoon is sensitive to the height of the Himalayas (Thompson and Pollard, 1995). Increasing the peak heights by 1–1.5 km to be in better agreement with actual heights produces a more realistic monsoon season with the correct timing of June through September.

The simulations in this study include an extensive ice sheet over southern Gondwana as a lower

boundary condition. The presence of permanent polar ice has been proposed as another mechanism for increased year-round equatorial rainfall (Ziegler et al., 1987). They propose that permanent polar high-pressure over this ice sheet would have suppressed seasonal excursions of the ITCZ and confined it to a narrow latitudinal belt creating a broad, year-round warm and wet equatorial climatic zone. The sensitivity of the seasonal excursions of the ITCZ to the presence and nature of the Gondwanan glaciation has been explored in an additional simulation (Otto-Bliesner, 1996). With no mountains (all land elevations set to sea level) and solar luminosity set to its present-day value (to keep the southern supercontinent of Gondwana free of permanent snowcover persisting over summer), there is no significant difference in either the seasonal excursions or latitudinal width of the belt of equatorial precipitation than in the simulation with a prescribed single ice sheet. Crowley et al. (1994) had similar results in their simulations with and without the Greenland ice sheet. These results counter the hypothesis that polar ice cover confines the Hadley cells and channels the equatorial rainy belt (Ziegler et al., 1987).

The general agreement between the geological record of extensive coals over a broad tropical latitudinal band in the Westphalian and our results when the Central Pangean Mountain Belt is included in a global climate model simulation as a lower boundary condition establishes the crucial role of this tropical mountain range in altering the tropical circulation patterns. Simulations exploring other mechanisms suggest that they can have an additive effect to that of the mountains. Crowley et al. (1995) found that equatorial precipitation during the late Carboniferous varied with Milankovitch orbital configuration. Coal deposits coincided with model-simulated temperate everwet conditions over Laurussia with better correlation when cold summer orbit conditions occurred in the Southern Hemisphere.

The robustness of the climatic response to tropical mountains will need to be tested further to understand its sensitivity to model prescriptions and parameterizations. Considerable uncertainty exists in the paleogeographic reconstructions (Heckel, 1995), representation of topographic roughness in climate models (Valdes, 1993), and atmospheric CO_2 (Berner, 1994) . In addition, the application of high-resolution (~50 km or less) regional climate models (Giorgi, 1995) , which can resolve patterns of precipitation and storm tracks that depend upon the detailed topography and coastlines, and proxy formation models (Wold and DeConto, 1998), which simulate the physical, chemical, and/or biological conditions necessary for the formation of climate-sensitive sediments, to paleoclimate problems can better define our understanding of the importance of tectonic controls on paleoclimate.

References

Berger, A.L., 1978, Long-term variations of caloric insolation resulting from the Earth's orbital elements, *Quat. Res.*, *9*, 139–167.

Berger, A.L., M.F. Loutre, and V. Dehant, 1989, Influence of the changing lunar orbit on the astronomical frequencies of pre-Quaternary insolation patterns, *Paleoceanography*, *4*, 555–564.

Berner, R.A., 1994, GEOCARB II: A revised model of atmospheric CO_2 over Phanerozoic time, *Am. J. Sci.*, *294*, 56–91.

Budyko, M.I., A.B. Ronov, and Y.L. Yanshin, 1987, *History of the Earth's Atmosphere*, Springer-Verlag, New York.

Caputo, M.V., and J.C. Crowell, 1985, Migration of glacial centers across Gondwana during the Paleozoic Era, *Geol. Soc. Am. Bull.*, *96*, 1020–1036.

Chaloner, W.G., and G.T. Creber, 1990, Do fossil plants give a climatic signal?, *J. Geol. Soc.*, *147*, 343–350.

Chervin, R.M., and S.H. Schneider, 1976, On determining the statistical significance of climate model experiments with general circulation models, *J. Atmos. Sci.*, *33*, 405–412.

Covey, C., and S.L. Thompson, 1989, Testing the effects of ocean heat transport on climate, *Palaeogeogr., Palaeoclimatol., Palaeoecol.*, *75*, 331–341.

Creber, G.T., and W.G. Chaloner, 1984, Influence of environmental factors on the wood structure of living and fossil trees, *Bot. Rev.*, *50*, 357–448.

Crowell, J.C., 1983, Ice ages recorded on Gondwanan continents, *Trans. Geol. Soc. S. Afr.*, *86*, 237–262.

Crowley, T.J., and S.K. Baum, 1991, Estimating Carboniferous sea-level fluctuations from Gondwanan ice extent, *Geology*, *19*, 975–977.

Crowley, T.J., S.K. Baum, and W.T. Hyde, 1991, Climate model comparison of Gondwana and Laurentide glaciations, *J. Geophys. Res.*, *96*, 9217–9226.

Crowley, T.J., K.-J. Yip, and S.K. Baum, 1994, Effect of altered Arctic sea ice and Greenland ice sheet cover

on the climate of the GENESIS general circulation model, *Glob. Planet. Change*, *9*, 275–288.

Crowley, T.J., K.-J. Yip, S.K. Baum, and S.B. Moore, 1995, Modeling Carboniferous coal formation, *Palaeoclimates: Data and Modelling, 2,* 159–177.

Endal, A.S., and S. Sofia, 1981, Rotation in solar-type stars, I, Evolutionary models for the spindown of the sun, *Astrophys. J.*, *243*, 625–640.

Freeman, K.H., and J.M. Hayes, 1992, Fractionation of carbon isotopes by phytoplankton and estimates of ancient CO_2 levels, *Global Biogeochem. Cycles, 6,* 185–198.

Garrels, R.M., and A. Lerman, 1984, Coupling of the sedimentary sulfur and carbon cycles — an improved model, *Am. J. Sci.*, *284*, 989–1007.

Giorgi, F., 1995, Perspectives for regional earth system modeling, *Glob. Planet. Change*, *10*, 23–42.

Hay, W.W., E.J. Barron, and S.L. Thompson, 1990, Results of global atmospheric circulation experiments on an Earth with a meridional pole-to-pole continent, *J. Geol. Soc. (London)*, *147*, 385–392.

Heckel, P.H., 1995, Glacial-eustatic base-level — Climatic model for Late Middle to Late Pennsylvanian coal-bed formation in the Appalachian basin, *J. Sedimen. Res.*, *B65*, 348–356.

Khramov, A.N., and V.P. Rodionov, 1980, Paleomagnetism and reconstruction of paleogeographic positions of the Siberian and Russian plates during the Late Proterozoic and Palaeozoic, *J. Geomagn. Geoelectr., 32*(suppl. III), SIII23–SIII37.

Kraus, J.U., C.R. Scotese, A.J. Boucot, and C. Xu, 1993, Lithologic indicators of climate: Preliminary report. Paleomap Project, Progress Report #33, Department of Geology, University of Texas, Arlington, Tex.

Kutzbach, J.E., 1994, Idealized Pangean climates: Sensitivity to orbital change, in *Pangea: Paleoclimate, Tectonics, and Sedimentation during Accretion, Zenith and Breakup of a Supercontinent*, G. D. Klein (ed.), pp. 41–56, Geological Society of America Special Paper 288, Boulder, Colo.

Kutzbach, J.E., P.J. Guetter, W.F. Ruddiman, and W.L. Prell, 1989, The sensitivity of climate to Late Cenozoic uplift in southeast Asia and the American southwest: Numerical experiments, *J. Geophys. Res.*, *94*, 18,393–18,407.

Kutzbach, J.E., and A.M. Ziegler, 1993, Simulation of Late Permian climate and biomes with an atmosphere-ocean model: Comparisons with observations, *Phil. Trans. R. Soc., Series B, 341*, 327–

340.

Kutzbach, J.E., W.L. Prell, and W.F. Ruddiman, 1993, Sensitivity of Eurasian climate to surface uplift of the Tibetan plateau, *J. Geol., 101*, 177–190.

Meehl, G.A., 1992, Effect of tropical topography on global climate, *Ann. Rev. Earth Planet. Sci., 20*, 85–112.

Mora, C.I., S.G. Driese, and L.A. Colarusso, 1996, Middle to late Paleozoic atmospheric CO_2 levels from soil carbonate and organic matter, *Science*, *271*, 1105–1107.

North, G.R., K.-J. Yip, L.-Y. Leung, and R.M. Chervin, 1992, Forced and free variations of the surface temperature field, *J. Clim.*, *5*, 227–239.

Otto-Bliesner, B.L., 1996, The initiation of a continental ice sheet in a global climate model (GENESIS), *J. Geophys. Res.*, *101*, 16,909–16,920.

Panofsky, H.A., and G.W. Brier, 1965., *Some Applications of Statistics to Meteorology*, Pennsylvania State University, University Park, Pa.

Parrish, J.M., J.T. Parrish, and A.M. Ziegler, 1986, Triassic paleogeography and paleoclimatology and implications for Therapsid distribution, in *The Ecology and Biology of Mammal-like Reptiles*, N. Hotton II, P. D. MacLean, J. J. Roth, and E. C. Roth (eds.), pp. 109–131, Smithsonian Institution Press, Washington, D.C.

Paterson, W.S.B., 1972, Laurentide ice sheets: Estimated volumes during late Wisconsin, *Rev. Geophys.*, *10*, 885–917.

Pollard, D., and S. L. Thompson, 1995, Use of a land-surface-transfer scheme (LSX) in a global climate model (GENESIS): The response to doubling stomatal resistance, *Glob. Planet. Change*, *10*, 129–161.

Raymond, A., P. H. Kelley, and C. B. Lutkin, 1989, Polar glaciers and life at the equator: The history of Dinantian and Namurian (Carboniferous) climate, *Geology*, *17*, 408–411.

Ronov, A.B., 1976, Global carbon geochemistry, volcanism, carbonate accumulation, and life, *Geoch. Int.*, *13*, 172–195.

Rowley, D. B., A. Raymond, J. T. Parrish, A. L. Lottes, C. R. Scotese, and A. M. Ziegler, 1985, Carboniferous paleogeographic, phytogeographic and paleoclimatic reconstructions, *Int. J. Coal Geol.*, *5*, 7–42.

Ruddiman, W. F., and J. E. Kutzbach, 1989, Forcing of late Cenozoic Northern Hemisphere climate by plateau uplift in southern Asia and the America west, *J. Geophys. Res.*, *94*, 18,409–18,427.

Ruddiman, W. F., and J. E. Kutzbach, 1990, Late Ceno-

zoic plateau uplift and climate change, *Trans. R. Soc. Edinburgh: Earth Sci., 81*, 301–314.

Scotese, C. R., 1994, Late Carboniferous paleogeographic map, Figure 3, in *Pangea: Paleoclimate, Tectonics, and Sedimentation During Accretion, Zenith and Breakup of a Supercontinent*, G. D. Klein (ed.), p. 6, Geological Society of America Special Paper 288, Boulder, Colo.

Semtner, A. J., Jr., 1976, A model for the thermodynamic growth of sea ice in numerical investigations of climate, *J. Phys. Oceanogr., 6*, 379–389.

Thompson, S. L., and D. Pollard, 1995, A global climate model (GENESIS) with a land-surface transfer scheme (LSX). Part 1: Present climate simulation, *J. Clim., 8*, 732–761.

Trewartha, G. T., and L. H. Horn, 1980, *An Introduction to Climate,* McGraw-Hill, New York.

Valdes, P., 1993, Atmospheric general circulation models of the Jurassic, *Phil. Trans. R. Soc. Lond., Series B, 341*, 317–326.

Van der Voo, R., 1993, *Paleomagnetism of Atlantis, Tethys, and Iapetus*, Cambridge University Press, Cambridge.

Veevers, J. M., and C. M. Powell, 1987, Late Paleozoic glacial episodes in Gondwanaland reflected in transgressive-regressive depositional sequences in Euramerica, *Geol. Soc. Am. Bull., 98*, 475–487.

Walker, J. C. G., P. B. Hays, and J. F. Kasting, 1981, A negative feedback mechanism for the long-term stabilization of Earth's surface temperature, *J. Geophys. Res., 86*, 9776–9782.

Wilson, K. M., D. Pollard, W. W. Hay, S. L. Thompson, and C. N. Wold, 1994, General circulation model simulations of Triassic climates: Preliminary results, in *Pangea: Paleoclimate, Tectonics, and Sedimentation During Accretion, Zenith and Breakup of a Supercontinent*, G. D. Klein (ed.), pp. 91–116, Geological Society of America Special Paper 288, Boulder, Colo.

Wold, C. N., and R. M. DeConto, 1998, Proxy formation model used to predict the locations of Late Cretaceous evaporites, in *The Evolution of Cretaceous Ocean/Climate Systems*, E. Barrera and C. Johnson (eds.), Geological Society of America Special Publication, (in press).

Yapp, C. J., and H. Poths, 1992, Ancient atmospheric CO_2 pressures inferred from natural goethites, *Nature, 355*, 342–344.

Ziegler, A. M., 1990, Phytogeographic patterns and continental configurations during the Permian Period, in *Palaeozoic Palaeogeography and Biogeography*, W. S. McKerrow and C. R. Scotese (eds.), pp. 363–379, *Geol. Soc. London Mem.*

Ziegler, A.M., C.R. Scotese, W.S. McKerrow, M.E. Johnson, and R.K. Bambach, 1979, Paleozoic paleogeography, *Annu. Rev. Earth Planet. Sci., 7*, 473–502.

Ziegler, A. M., D. B. Rowley, A. L. Lottes, D. L. Sahagian, M. L. Hulver, and T. C. Gierlowski, 1985, Paleogeographic interpretation: With an example from the Mid-Cretaceous, *Annu. Rev. Earth Planet. Sci., 13*, 385–425.

Ziegler, A. M., A. Raymond, T. C. Gierlowski, M. A. Horrell, D. B. Rowley, and A. L. Lottes, 1987, Coal, climate, and terrestrial productivity: The present and early Cretaceous compared, in *Coal and Coal-Bearing Strata: Recent Advances*, A. C. Scott (ed.), pp. 25–49, Geol. Soc. London Spec. Pub., London.